F_L proton structure function from the unified DGLAP/BFKL approach

K. Golec-Biernat[1,2,*] and A. M. Staśto[3,4,1,†]

[1]*Institute of Nuclear Physics PAN, Kraków, Poland*
[2]*Institute of Physics, Rzeszów University, Rzeszów, Poland*
[3]*Penn State University, Physics Department, University Park, Pennsylvania 16802, USA*
[4]*RIKEN Center, Brookhaven National Laboratory, Upton, New York 11973, USA*

We compute the longitudinal proton structure function F_L from the k_T factorization scheme, using the unified DGLAP/BFKL resummation approach at small x for the unintegrated gluon density. The differences between the k_T factorization, collinear factorization, and dipole approaches are analyzed and discussed. The comparisons with the DESY collider HERA data are made and predictions for the proposed large hadron-electron collider are also provided.

I. INTRODUCTION

The longitudinal nucleon structure function F_L, measured in the deep inelastic lepton-nucleon scattering, is proportional to the cross section for the interaction of the longitudinally polarized virtual photon with a nucleon. This observable is of particular interest since it is directly sensitive to the nucleon gluon distribution. In the naive quark-parton model F_L vanishes (the Callan-Gross relation). This is due to the quark spin $1/2$ and the fact that the struck quark has limited transverse momentum in the naive parton model. In the QCD improved parton model, however, the gluon interactions cause the average quark transverse momentum $\langle \kappa_T^2 \rangle$ to grow with increasing value of the (minus) photon virtuality Q^2. As a result, F_L acquires a nonzero leading twist contribution proportional to $\alpha_s(Q^2)$. At small values of the Bjorken variable x, F_L is driven mainly by gluons through the transition $g \to q\bar{q}$. Therefore, it can be used for the extraction of the gluon distribution in a nucleon providing a crucial test of the validity of perturbative QCD in this kinematical range.

The experimental determination of F_L is in general difficult and requires a measurement of the inelastic cross section at the same values of x and Q^2 but for different center-of-mass energy of the incoming beams. This was achieved at the DESY electron-proton collider HERA by changing the proton beam energy with the lepton beam energy fixed. The structure function F_L was measured both by the H1 [1] and ZEUS [2] Collaborations in the Q^2 range of 12–90 and 24–110 GeV^2, respectively.

At small x, the nucleon structure functions receive large logarithmic corrections coming from resummation of large powers of $\alpha_s \ln 1/x$. This procedure goes beyond the standard collinear factorization and is achieved by the use of the k_T factorization formalism [3,4] with the unintegrated

gluon density found as a solution to the Balitsky-Fadin-Kuraev-Lipatov (BFKL) [5–7] or Ciafaloni-Catani-Fiorani-Marchesini (CCFM) evolution equations [8–11]. Since the small x expansion receives large corrections at higher orders, resummation at small x is in general necessary in order to obtain predictions which are in agreement with data.

The objective of this paper is the calculation of F_L within the k_T factorization formalism using the unintegrated gluon density obtained from the Kwieciński-Martin-Staśto (KMS) approach [12], which provides a convenient framework for the unification of the conventional Dokshitzer-Gribov-Lipatov-Altarelli-Parisi (DGLAP) [13–15] and small x BFKL evolution equations. From the point of view of the small x hierarchy, the KMS approach includes important effects of higher order resummation. In addition, we systematically analyze the relation between this approach and the collinear and dipole approaches, investigating the role of different contributions to F_L in various kinematical regions. We especially emphasize the role of the exact gluon kinematics in the k_T factorization formulas and demonstrate numerically that this kinematics has a sizable effect on the predictions for F_L, and thus, on the extracted gluon density. We compare our computations with the experimental data at small x from the H1 [1] and ZEUS [2] Collaborations.

The paper is organized as follows. In Sec. II we recall the k_T factorization formalism for the longitudinal structure function. In Sec. III we review the unified BFKL/DGLAP approach for the unintegrated gluon density which includes important resummation effects at small x. In Sec. IV we discuss the relation of the k_T factorization with the collinear and dipole approaches. In Sec. V we present a systematic numerical analysis of the various approaches and compare them with the HERA data, as well as provide the extrapolations to the LHeC (large hadron-electron collider [16]) energies. In the last section we summarize our conclusions.
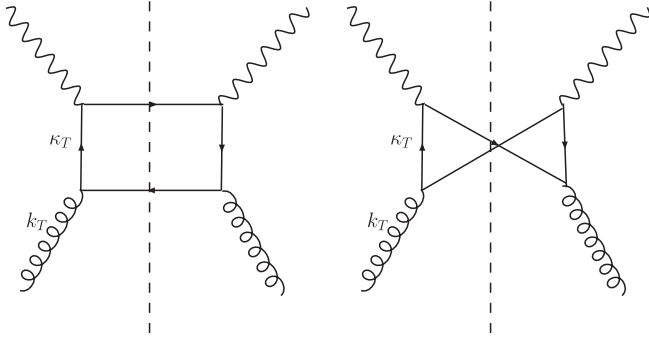
_____
*golec@ifj.edu.pl
†astasto@phys.psu.edu

FIG. 1. Quark box diagrams in the photon-gluon fusion process used in the k_T factorization formula.

II. F_L FROM THE k_T FACTORIZATION APPROACH

In the limit of the high center-of-mass energy, or equivalently at small values of Bjorken x, the nucleon structure functions can be computed from the k_T factorization approach [3,4]. Basic diagrams for the boson-gluon fusion which are taken into account in the high energy limit are depicted in Fig. 1. The gluon is off shell with its virtuality dominated by the transverse momentum $k_T \equiv k$ (see Fig. 1). Since we are interested in F_L, the photon is longitudinally polarized. Thus, in the k_T factorization approach the longitudinal structure function is then given by

$$F_L(x, Q^2) = 2\frac{Q^4}{\pi^2}\sum_q e_q^2 \int \frac{dk^2}{k^4} \int_0^1 d\beta \int d^2\kappa' \alpha_s(\mu^2)$$
$$\times \beta^2(1 - \beta)^2 \frac{1}{2}\left(\frac{1}{D_{1q}} - \frac{1}{D_{2q}}\right)^2 f\left(\frac{x}{z}, k^2\right), \quad (1)$$

where the denominators D_{1q} and D_{2q} read

$$D_{1q} = \kappa^2 + \beta(1 - \beta)Q^2 + m_q^2, \quad (2)$$

$$D_{2q} = (\boldsymbol{\kappa} - \boldsymbol{k})^2 + \beta(1 - \beta)Q^2 + m_q^2, \quad (3)$$

the quark transverse momentum $\kappa_T \equiv \boldsymbol{\kappa}$, the shifted transverse momentum is given by $\boldsymbol{\kappa}' = \boldsymbol{\kappa} - (1 - \beta)\boldsymbol{k}$, and the argument of the unintegrated gluon density $f(x/z, k^2)$ is defined to be

$$\frac{x}{z} \equiv x_g \equiv x\left(1 + \frac{\kappa'^2 + m_q^2}{\beta(1 - \beta)Q^2} + \frac{k^2}{Q^2}\right). \quad (4)$$

The variable β is the corresponding Sudakov parameter appearing in the quark momentum decomposition,

$$\kappa = x_q p' - \beta q' + \boldsymbol{\kappa} \quad (5)$$

$$x_q = x\left(1 + \frac{m_q^2 + \boldsymbol{\kappa}'}{(1 - \beta)Q^2}\right), \quad (6)$$

with the following lightlike base vectors:

$$p' = p - \frac{M^2 x}{Q^2}q, \qquad q' = q + xp, \quad (7)$$

where M denotes the nucleon mass, m_q is the quark mass which we keep nonzero only for charm quark, p is the target-proton four-momentum, and q is the virtual photon four-momentum. The argument in the strong coupling constant is taken to be

$$\mu^2 = \kappa'^2 + k^2 + m_q^2. \quad (8)$$

The integration over the gluon virtuality k^2 in Eq. (1) needs special care in the low momenta region, $k^2 < k_0^2 \simeq 1$ GeV^2. We will discuss this important element of our presentation in the forthcoming sections.

The function $f(y, k^2)$ is the unintegrated gluon distribution, which in the small x limit is related to the conventional (integrated) gluon distribution $g(y, \mu^2)$ by

$$yg(y, \mu^2) = \int^{\mu^2} \frac{dk^2}{k^2} f(y, k^2). \quad (9)$$

The integration limits in (1) are constrained by the condition $x_g < 1$ while the condition $x_g > x$ is automatically satisfied from Eq. (4). We note that in the strict high energy limit the argument of the unintegrated gluon distribution would be set to the Bjorken x. This is also the usual procedure in the dipole picture approach which we discuss in Sec. IV. Here, we take into account the effects of exact kinematics which results in the shift of the gluon x_g to larger values than x. This is related to the fact that the energy needed to produce the $q\bar{q}$ pair is non-negligible even when the total center-of-mass energy is very large. Although this effect is nonleading in the leading logarithmic small x approximation, it is nevertheless numerically quite important, as we will illustrate in Sec. V.

It also has been shown in the dipole picture that by including the exact kinematics in the argument of the gluon distribution, the transverse size of the quark-antiquark dipole is no longer conserved [17,18] (see Sec. IV B).

III. UNIFIED DGLAP AND BFKL EQUATIONS

The main input to the k_T factorization formula is the unintegrated gluon distribution $f(y, k^2)$. At small x, this distribution can be found from the solution to the BFKL [5–7] or the CCFM equations [8–11]. These equations give predictions for the unintegrated gluon density as a function of the transverse momentum squared k^2 and x (and also an external scale Q in the case of the CCFM equation) provided $x \ll 1$. A more rigorous approach which includes the operator definitions of unintegrated gluon densities is presented in [19]. Here, we will use the unintegrated density obtained from the solution to the set of unified BFKL and DGLAP equations, which includes the small x resummation effects. The full formalism, called the KMS approach, was constructed in [12] and here we only review main elements of this approach.

A. Equation for the unintegrated gluon density

In the KMS approach [12] one constructs the evolution equation for the unintegrated gluon distribution function which includes the leading order BFKL kernel with the kinematical constraint and the DGLAP part of the splitting function. The solution to the leading order BFKL equation is well known [20], giving very fast growth of the gluon density with the decreasing value of x. It can be recast into the symbolic form:

$$f(x, k^2) \sim x^{-\lambda}, \tag{10}$$

where $\lambda \simeq 0.5$ is the so-called hard Pomeron intercept. This fast growth was shown to be incompatible with the experimental data which exhibit an effective intercept $\lambda \simeq 0.3$.

The next-to-leading corrections to the BFKL equation turned out to be very large [21–23] and it became imme-

diately apparent that additional resummations are necessary. In the KMS approach one uses the leading logarithmic approximation for the BFKL kernel but with substantial modifications. One of them is the kinematical constraint [24,25] which accounts for a large portion of the next-to-leading order corrections. It is important to stress that this constraint goes beyond the next-to-leading order in logarithms of x, and is responsible for partial resummation of the small x series [26]. Another modification in the KMS approach is a nonsingular part in $1/z$ of the splitting function P_{gg} in the BFKL kernel in addition to the already included singular part. In a series of papers [27–29] (see also [30–35]) it was shown in detail how these modifications generate higher order terms in the small x expansion.

The final equation in the KMS approach, which takes into account all the modifications mentioned above, has the following form:

$$f(x, k^2) = \tilde{f}^{(0)}(x, k^2) + \bar{\alpha}_S(k^2)k^2 \int_x^1 \frac{dz}{z} \int_{k_0^2} \frac{dk'^2}{k'^2} \left\{ \frac{f(\frac{x}{z}, k'^2)\Theta(\frac{k^2}{z} - k'^2) - f(\frac{x}{z}, k^2)}{|k'^2 - k^2|} + \frac{f(\frac{x}{z}, k^2)}{[4k'^4 + k^4]^{1/2}} \right\}$$
$$+ \bar{\alpha}_S(k^2) \int_x^1 \frac{dz}{z} \left(\frac{z}{6} P_{gg}(z) - 1 \right) \int_{k_0^2}^{k^2} \frac{dk'^2}{k'^2} f\left(\frac{x}{z}, k'^2\right) + \frac{\alpha_S(k^2)}{2\pi} \int_x^1 dz P_{gq}(z) \Sigma\left(\frac{x}{z}, k^2\right), \tag{11}$$

where the strong coupling constant $\bar{\alpha}_s \equiv \alpha_s N_c / \pi$. The first term on the right-hand side is the nonperturbative input to be specified below, while the second term contains the leading logarithmic BFKL kernel with the kinematical constraint given by the theta function. The third term contains the DGLAP splitting function $P_{gg}(z)$ without the singular term in z, and the last term is the contribution from the quark to gluon transition with Σ being the singlet quark distribution. The input function for this integral equation is chosen to be

$$\tilde{f}^{(0)}(x, k^2) = \frac{\alpha_S(k^2)}{2\pi} \int_x^1 dz P_{gg}(z) \frac{x}{z} g\left(\frac{x}{z}, k_0^2\right). \tag{12}$$

Note that the special form of the input is dictated by the fact that Eq. (11) only involves $f(x, k^2)$ in the perturbative domain, $k^2 > k_0^2$, where k_0^2 is a nonperturbative cutoff taken to be equal $k_0^2 = 1$ GeV^2. The gluon input (12) is provided by the conventional gluon distribution $xg(x, k_0^2)$. This guarantees consistency with the DGLAP evolution equations since the input in both approaches is exactly of the same. In this way, the necessity of parametrizing the unintegrated

gluon distribution in the nonperturbative regime, $k^2 < k_0^2$, is avoided.

B. Equation for the singlet quark density

In the KMS approach the equation for the unintegrated gluon density was supplemented by the second equation for the quark density. These two equations formed the coupled system of equations (similarly to the DGLAP equations) for the functions $f(x, k^2)$ and $\Sigma(x, k^2)$. The sea quark contribution was evaluated from the k_T factorization theorem at small x,

$$S_q^{(k)}(x, Q^2) = \int_x^1 \frac{dz}{z} \int \frac{dk^2}{k^2} S_q^{(\text{box})}(z, k^2, Q^2) f(x_g, k^2), \tag{13}$$

where $S_q^{(\text{box})}$ describes the quark box contributions, shown in Fig. 1, which implicitly includes the integration over the quark transverse momentum $\boldsymbol{\kappa}$. The explicit expression for (13) reads

$$S_q^{(k)}(x, Q^2) = \frac{Q^2}{4\pi^2} \int \frac{dk^2}{k^4} \int_0^1 d\beta \int d^2\kappa' \alpha_S \left\{ [\beta^2 + (1-\beta)^2] \left(\frac{\boldsymbol{\kappa}}{D_{1q}} - \frac{\boldsymbol{\kappa} - \boldsymbol{k}}{D_{2q}} \right)^2 + [m_q^2 + 4Q^2\beta^2(1-\beta)^2] \left(\frac{1}{D_{1q}} - \frac{1}{D_{2q}} \right)^2 \right\}$$
$$\times f\left(\frac{x}{z}, k^2\right) \Theta\left(1 - \frac{x}{z}\right), \tag{14}$$

where the quantities κ', D_{1q}, D_{2q}, and x_g were defined in Sec. II.

The singlet quark momentum distribution contains both the sea and valence quarks. The contribution to the singlet quark distribution was calculated differently depending on the region of the transverse momenta. There are three regions of interest for k^2 and κ'^2:

(1) nonperturbative: k^2, $\kappa'^2 < k_0^2$,
(2) strongly ordered with low gluon transverse momenta: $k^2 < k_0^2 < \kappa'^2$,
(3) perturbative: $k^2 > k_0^2$.

In the nonperturbative region, the sea contribution is assumed to be dominated by the soft-Pomeron exchange. This part is parametrized phenomenologically in the following form:

$$S^{(\text{soft})}(x) = S_u^P + S_d^P + S_s^P, \tag{15}$$

with the soft-Pomeron contribution

$$S_u^P = S_d^P = 2S_s^P = C_P x^{-0.08}(1 - x)^8. \tag{16}$$

The second contribution comes from the region of small transverse momenta of the gluon, $k^2 < k_0^2 < \kappa'^2$. In this

region the strongly ordered approximation for the quark-gluon transition is applied and the relevant contribution is given by the following formula:

$$S^{(\text{coll})}(x, Q^2) = \int_x^1 \frac{dz}{z} S_q^{(\text{box})}(z, k^2 = 0, Q^2) \frac{x}{z} g\left(\frac{x}{z}, k_0^2\right), \tag{17}$$

where the on-shell approximation, $k^2 = 0$, is applied to evaluate $S_q^{(\text{box})}$.

In the perturbative domain, $k^2 > k_0^2$, the quark contribution is evaluated from the k_T factorization formula. The final expression for the singlet quark distribution is taken to be the sum of the contributions from the three discussed regions

$$\Sigma = (S_{uds}^{(\text{soft})} + S_{uds}^{(\text{coll})} + S_{uds}^{(k)}) + (S_c^{(\text{coll})} + S_c^{(k)}) + V. \tag{18}$$

Note that for the charm evaluation we did not use the soft contribution since we assume that charm is generated dynamically from gluons and that there is no soft or nonperturbative charm contribution.

Using the k_T factorization and all the terms discussed above, one finds the final equation for the singlet distribution Σ in the KMS approach:

$$\Sigma(x, k^2) = S^{(\text{soft})}(x) + \sum_q \int_x^a \frac{dz}{z} S_q^{(\text{box})}(z, k'^2 = 0, k^2; m_q^2) \frac{x}{z} g\left(\frac{x}{z}, k_0^2\right) + V(x, k^2)$$

$$+ \sum_q \int_{k_0^2}^\infty \frac{dk'^2}{k'^2} \int_x^1 \frac{dz}{z} S_q^{(\text{box})}(z, k'^2, k^2; m_q^2) f\left(\frac{x}{z}, k'^2\right) + \int_{k_0^2}^{k^2} \frac{dk'^2}{k'^2} \frac{\alpha_S(k'^2)}{2\pi} \int_x^1 dz P_{qq}(z) S_{uds}\left(\frac{x}{z}, k'^2\right), \tag{19}$$

where $S^{(\text{soft})}(x)$ is given by Eq. (15) and the *uds* subscript indicates that the additional $S \rightarrow S$ term is only included for the light quarks. Equations (19) and (11) form a set of equations to be solved in the KMS approach.

The final formula used for the calculation of the longitudinal structure function F_L from the k_T factorization formalism with the KMS approach reads

$$F_L(x, Q^2) = \frac{Q^4}{\pi^2} \sum_q e_q^2 \int \frac{dk^2}{k^4} \theta(k^2 > k_0^2) \int_0^1 d\beta \int d^2\kappa' \alpha_s(\mu^2) \beta^2 (1 - \beta)^2 \left(\frac{1}{D_{1q}} - \frac{1}{D_{2q}}\right)^2 f(x_g, k^2)$$

$$+ \frac{\alpha_s(Q^2)}{\pi} \left\{ \frac{4}{3} \int_x^1 \frac{dy}{y} \left(\frac{x}{y}\right)^2 F_2(y, Q^2) + \sum_q e_q^2 \int_x^1 \frac{dy}{y} \left(\frac{x}{y}\right)^2 \left(1 - \frac{x}{y}\right) y g(y, k_0^2) \right\}, \tag{20}$$

where the cutoff for the gluon momentum $k_0^2 = 1$ GeV^2 and the nonperturbative input was taken to be

$$y g(y, k_0^2) = N(1 - y)^\beta \tag{21}$$

with the parameters $N = 1.57$ and $\beta = 2.5$, which were found from a fit to the HERA data on the structure function F_2, using the same approach. In the forthcoming, we will discuss in detail the relation of the k_T factorization formula (20) to those from other approaches.

It is interesting to see what is the magnitude of the separate contributions to F_L in Eq. (20). In Fig. 2 we

show the breakdown of F_L into the contributions from gluons from the boson-gluon box (first term), quarks (second term) and the nonperturbative gluon input (third term). The nonperturbative input stays nearly constant as a function of x and Q^2. At low x the dominant contribution is from the gluon density in the k_T factorization framework. However, this contribution is small at $x > 0.01$ and at small values of Q^2. This is due to the kinematic effects since phase space for the gluon emissions shrinks in this regime. On the other hand, the quark contribution is non-negligible in the same regime.
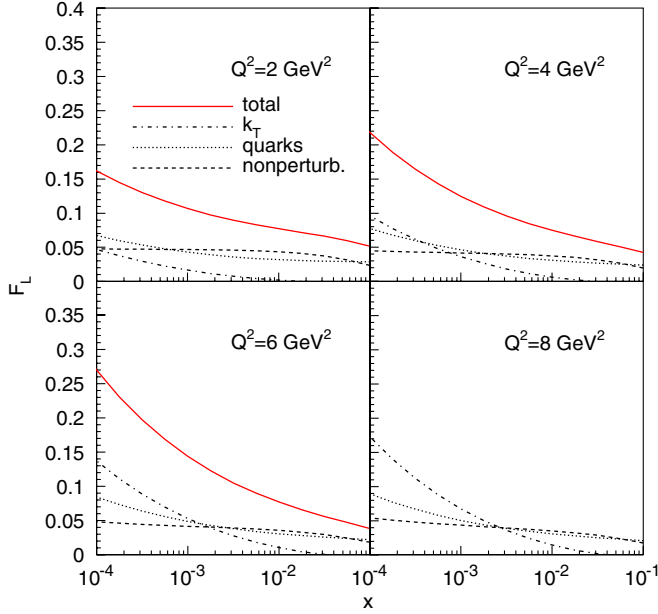
FIG. 2 (color online). F_L from the k_T factorization approach. Dashed-dotted (black) line: contribution from the boson-gluon fusion box with gluon transverse momenta $k > k_0$; dashed (black) line: nonperturbative input from the gluons via collinear formula; and dotted (black) line: contribution from the quarks. Solid (red) line is the sum of all contributions. Gluon kinematics is exact.

IV. RELATION OF THE k_T FACTORIZATION TO OTHER APPROACHES

A. Relation to the collinear factorization approach

The standard collinear factorization formula for the longitudinal structure function reads

$$F_L(x, Q^2) = \frac{\alpha_s(Q^2)}{\pi} \left[2 \sum_q e_q^2 \int_x^1 \frac{dy}{y} \left(\frac{x}{y}\right)^2 \left(1 - \frac{x}{y}\right) yg(y, Q^2) \right.$$
$$\left. + \frac{4}{3} \int_x^1 \frac{dy}{y} \left(\frac{x}{y}\right)^2 F_2(x, Q^2) \right], \qquad (22)$$

where quark masses in this formula are neglected. Thus, F_L has two contributions: originating from quarks and proportional to F_2, and from gluons and proportional to the integrated gluon distribution $g(y, Q^2)$.

It is instructive to illustrate that the on-shell limit of the k_T factorization formula (1) is compatible with formula (22). By the on-shell limit we mean the approximation in which the transverse momentum of the gluon k^2 is much smaller than the virtuality of the photon, $k^2 \ll Q^2$. To this aim, we start by expanding the expression under the integral in Eq. (1),

$$\frac{1}{2} \left(\frac{1}{D_{1q}} - \frac{1}{D_{2q}} \right)^2, \qquad (23)$$

in powers of k^2/Q^2. We retain only the leading term, proportional to k^2, and drop all the higher powers of k^2.

Explicit expressions for the denominators D_{1q} and D_{2q} read

$$D_{1q} = \kappa'^2 + 2(1 - \beta)\boldsymbol{\kappa}' \cdot \boldsymbol{k} + (1 - \beta)^2 k^2$$
$$+ \beta(1 - \beta)Q^2 + m_q^2,$$
$$D_{2q} = \kappa'^2 - 2\beta\boldsymbol{\kappa}' \cdot \boldsymbol{k} + \beta^2 k^2 + \beta(1 - \beta)Q^2 + m_q^2.$$

After expanding the denominators in k^2 we obtain

$$\frac{1}{D_{1q}} = \frac{1}{D_q} - \frac{2(1 - \beta)\boldsymbol{\kappa}' \cdot \boldsymbol{k}}{D_q^2} + O(k^2),$$
$$\frac{1}{D_{2q}} = \frac{1}{D_q} + \frac{2\beta\boldsymbol{\kappa}' \cdot \boldsymbol{k}}{D_q^2} + O(k^2),$$

where

$$D_q = \kappa'^2 + \beta(1 - \beta)Q^2 + m_q^2 \qquad (24)$$

is independent of the gluon transverse momentum $\boldsymbol{k}$. Here, we need to keep only terms linear in k. Therefore, expression (23) to the first order in k^2 reads

$$\left(\frac{1}{D_{1q}} - \frac{1}{D_{2q}} \right)^2 = \frac{4\cos^2\phi \, \kappa'^2 k^2}{D_q^4}. \qquad (25)$$

The integration $d^2\kappa'$ can be written as $\frac{1}{2} d\kappa'^2 d\phi$ and one can perform the azimuthal integration over the angle ϕ. The dependence on k^2 is now only in the unintegrated gluon distribution. Since we have assumed the strong ordering in the transverse momenta, we can easily perform this integration using the following definition:

$$yg(y, \mu^2) \equiv \int^{\mu^2} \frac{dk^2}{k^2} f(y, k^2), \qquad (26)$$

where the scale $\mu^2 \sim Q^2$. Note that, formally the integration over the k in Eq. (1) is over all scales. However, we expand the k_T factorization formula for small values of k^2/Q^2 and assume that transverse momenta are small. Therefore, using relation (26), we can rewrite the approximate form as

$$F_L^{\text{(onshell)}}(x, Q^2) = 2 \frac{Q^4}{\pi} \sum_q e_q^2 \int_0^1 d\beta \int d\kappa'^2 \alpha_s(Q^2)$$
$$\times \beta^2 (1 - \beta)^2 \frac{\kappa'^2}{D_q^4} yg(y, \mu^2), \qquad (27)$$

where now

$$y \equiv x \left(1 + \frac{\kappa'^2 + m_q^2}{\beta(1 - \beta)Q^2} \right), \qquad (28)$$

since we have dropped the ratio k^2/Q^2 in x_g [see Eq. (4)]. It is convenient to change the integration variables in Eq. (27) from κ'^2 to y,

$$\kappa'^2 = \beta(1 - \beta)Q^2(\tfrac{y}{x} - 1) - m_q^2, \qquad (29)$$

$$D_q = \beta(1 - \beta)Q^2\frac{y}{x}, \tag{30}$$

and carefully set the integration limits. Using relation (29) we can write the inequality

$$\beta(1 - \beta)Q^2(\tfrac{y}{x} - 1) - m_q^2 > 0, \tag{31}$$

and since $1 > \beta > 0$, we have

$$\frac{1}{4} > \beta(1 - \beta) > \frac{m_q^2 x}{Q^2(y - x)}. \tag{32}$$

From inequality (32) we obtain the lower limit for y

$$y > x\left(1 + \frac{4m_q^2}{Q^2}\right). \tag{33}$$

It is now convenient to make another change of variables:

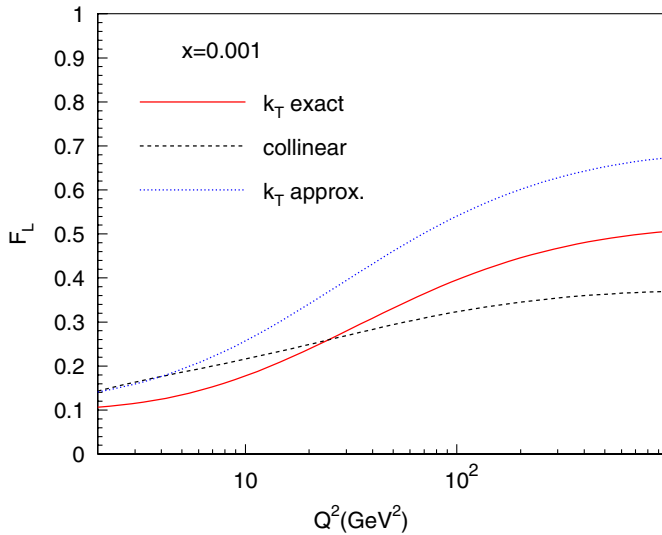$$\beta = \tfrac{1}{2} + \lambda, \tag{34}$$

and using inequality (32), we finally obtain

$$-\sqrt{\frac{1}{4} - \frac{m_q^2 x}{Q^2(y - x)}} < \lambda < \sqrt{\frac{1}{4} - \frac{m_q^2 x}{Q^2(y - x)}}. \tag{35}$$

As a result, we obtain the following expression for the on-shell limit of the k factorization formula:

$$F_L^{(\text{onshell})}(x, Q^2) = 2\sum_q e_q^2 \left[J_q^{(1)} - 2\frac{m_q^2}{Q^2} J_q^{(2)} \right], \tag{36}$$

where

$$J_q^{(1)} = \frac{\alpha_s}{\pi} \int_{\bar{x}_q}^1 \frac{dy}{y} \left(\frac{x}{y}\right)^2 \left(1 - \frac{x}{y}\right) \sqrt{1 - \frac{4m_q^2 x}{Q^2(y - x)}} yg(y, Q^2), \tag{37}$$

and

$$J_q^{(2)} = \frac{\alpha_s}{\pi} \int_{\bar{x}_q}^1 \frac{dy}{y} \left(\frac{x}{y}\right)^3 \ln\left[\frac{1 + \sqrt{1 - \frac{4m_q^2 x}{Q^2(y - x)}}}{1 - \sqrt{1 - \frac{4m_q^2 x}{Q^2(y - x)}}}\right] yg(y, Q^2) \tag{38}$$

with the lower cutoff on the integration equal to

$$\bar{x}_q = x\left(1 + \frac{4m_q^2}{Q^2}\right). \tag{39}$$

Formula (36) together with Eqs. (37) and (38) is the on-shell approximation derived from the k_T factorization in the presence of quark masses. In this derivation we also assumed that the argument of the coupling constant is equal to the external scale $\mu^2 \simeq Q^2$. It is straightforward to verify that the above expressions coincide with the gluonic contribution of the standard massless collinear formula (22) in the case when the quark masses vanish. Therefore, the collinear formula arises as a leading twist part of the k_T factorization formula, and the second term in Eq. (36) contains a part of the higher twist contribution proportional to $1/Q^2$.

Let us emphasize that in order to obtain the limit of the k_T factorization formula consistent with the collinear factorization, it was crucial to take the exact kinematics for the argument of the gluon density, x_g [see formulas (1), (4),
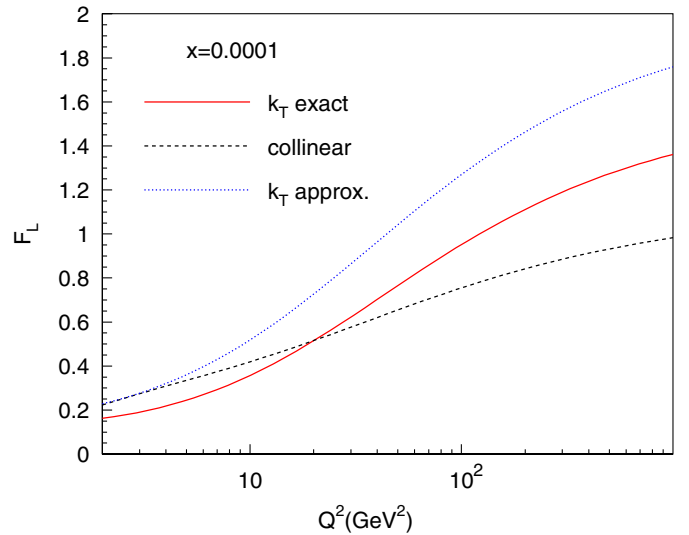

FIG. 3 (color online). Comparison between the k_T factorization and collinear factorization predictions for F_L as a function of Q^2 for two values of x: 10^{-3}, (left) and 10^{-4} (right). The solid lines are the k_T factorization prediction with exact kinematics, Eq. (20), while the dotted lines correspond to the dipole approximation, that is $x_g \rightarrow x$ in the gluon density. The dashed lines show the collinear factorization predictions, Eqs. (37) and (38).

and (28)]. The numerical relevance of the above substitution in the k_T factorization formula is shown in Fig. 3. In this figure we show the Q^2 dependence of F_L obtained within the k_T factorization approach with and without the exact kinematics, as well as the computation within the collinear approach. The differences between the collinear and k_T factorization approaches are not significant although there is distinctive difference in the slope of the Q^2 dependence. On the other hand, the differences due to the exact gluon kinematics are quite substantial and persist even in the small x regime.

B. Relation to the dipole approach

The dipole representation for the inclusive cross section can be computed from the k_T factorization formula. It is obtained after the Fourier transformation of expression (1) from the space of quark transverse momenta $\boldsymbol{\kappa}$ into the space of the transverse coordinates, $\mathbf{r}$. It is important to note that one also needs to perform the small x approximation in the argument of the gluon density in formula (1),

$$x_g \to x. \tag{40}$$

This is obviously justified only in the limit of very small x. In this way the Fourier integrals over the $\boldsymbol{\kappa}$ variable in (1) can be easily performed.

In the case of the longitudinal structure function,

$$F_L = \frac{Q^2}{4\pi^2 \alpha_{\mathrm{em}}} \sigma_L, \tag{41}$$

where the longitudinally polarized photon-proton cross section σ_L reads

$$\sigma_L = \frac{\alpha_{\mathrm{em}}}{\pi} \sum_q e_q^2 \int d^2\boldsymbol{r} \int_0^1 d\beta 4Q^2 \beta^2 (1-\beta)^2 K_0^2(\bar{Q}r)$$
$$\times \int \frac{d^2\boldsymbol{k}}{k^4} \alpha_s f(x, k^2)(1 - e^{-i\boldsymbol{r}\cdot\boldsymbol{k}})(1 - e^{i\boldsymbol{r}\cdot\boldsymbol{k}}). \tag{42}$$

Here $\boldsymbol{k}$ is the gluon transverse momentum, the variable

$$\bar{Q}^2 = \beta(1-\beta)Q^2 + m_q^2, \tag{43}$$

K_0 is the Bessel function, and $\boldsymbol{r}$ is the transverse size of the $q\bar{q}$ pair. The expression with the integral over $\boldsymbol{k}$ in Eq. (42) is proportional to the dipole-proton cross section, $\hat{\sigma}$, which characterizes the interaction of the $q\bar{q}$ color dipole with the proton

$$\hat{\sigma}(x, \boldsymbol{r}) \equiv \frac{2\pi}{3} \int \frac{d^2\boldsymbol{k}}{k^4} \alpha_s f(x, k^2)(1 - e^{-i\boldsymbol{r}\cdot\boldsymbol{k}})(1 - e^{i\boldsymbol{r}\cdot\boldsymbol{k}}). \tag{44}$$

Notice that such a Fourier transformation is only possible if the substitution (40) is done. Otherwise, by including the exact kinematics in the argument of the gluon distribution, the transverse size of the quark-antiquark dipole is no longer conserved [17,18,36].

In [37] a systematic analysis of the twist expansion (i.e. the expansion in powers of $1/Q^2$) in the dipole model approach was performed. Using the saturation model [38] for the dipole-proton cross section, a complete hierarchy of the twist series has been established. The analysis has been extended in [39] to a saturation model which includes the DGLAP evolution [36]. The higher twist terms are proportional to the nonlinear terms in the gluon density. Consequently, the leading twist part is the term which is linear in the gluon density. The leading twist-2 part in the dipole picture in the case of the cross section for the longitudinally polarized photon reads [37]

$$\sigma_L^{(\mathrm{twist}\text{-}2)} = \frac{4\pi\alpha_{\mathrm{em}}}{3} \sum_q e_q^2 \frac{\alpha_s xg(x, Q^2)}{Q^2}, \tag{45}$$

or for the longitudinal structure function

$$F_L^{(\mathrm{twist}\text{-}2)} = \frac{1}{3\pi} \sum_q e_q^2 \alpha_s xg(x, Q^2). \tag{46}$$

As we noted above, the dipole picture can be recovered from the k_T factorization formula (1) by taking the high energy limit and making the substitution (40). In order to recover the leading twist-2 expression in the high energy limit, it is therefore enough to consider the gluon part of the collinear formula (22) and replace the integrated gluon density by

$$yg(y, Q^2) \to xg(x, Q^2), \tag{47}$$

which allows to pull it outside the integral. The integral over y can be then performed exactly

$$\int_x^1 \frac{dy}{y}\left(\frac{x}{y}\right)^2\left(1 - \frac{x}{y}\right) = \frac{1}{6} + \frac{1}{6}x^2(2x - 3) \simeq \frac{1}{6},$$

where we assume that $x \ll 1$. Combining the above result with Eq. (22), we obtain the twist-2 contribution to F_L in the small x approximation given by Eq. (46). Therefore, the leading twist term from the dipole approach is actually an approximation to the leading twist collinear factorization formula (22). In Fig. 4 we demonstrate numerically that the values of F_L obtained from Eq. (46) are larger than those from the collinear factorization formula.

Summarizing, we have demonstrated how the collinear and dipole approaches are related to the k_T factorization formula (1). The collinear formula is obtained upon expanding the k_T factorization formula in powers of k^2/Q^2 and retaining the lowest order in this expansion. The exact gluon kinematics has to be taken into account in that procedure. On the other hand, the dipole approach is obtained from the k_T factorization expression in the limit when x is very small, which amounts to approximating the gluon longitudinal momentum fraction x_g by the Bjorken x.
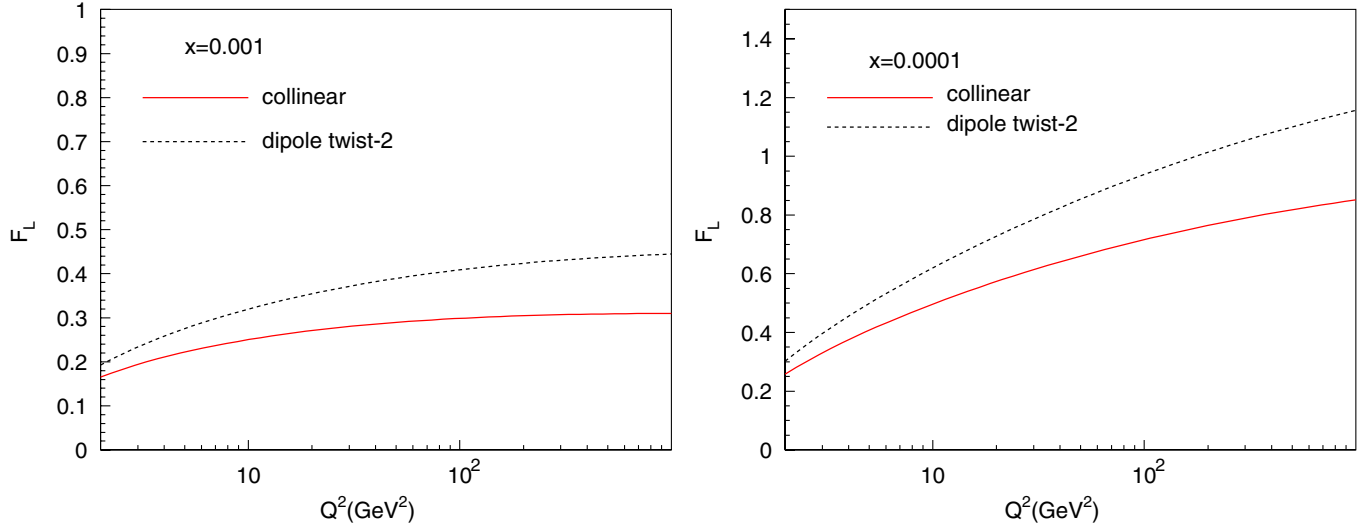
FIG. 4 (color online).   Comparison between the collinear factorization formula (22) with only the gluon term and massless quarks (solid lines) and the dipole twist-2 predictions (dashed lines) as a function of Q^2 for two values of x: 10^{-3} (left) and $x = 10^{-4}$ (right).

V. COMPARISON WITH THE HERA DATA

We start our numerical analysis by comparing the calculations of the longitudinal structure function F_L performed within the collinear formalism and the k_T factorization formalism with and without the exact kinematics. To be precise, for the collinear calculation we use the formulas (36)–(38) with the light quark masses set to

zero and the charm quark mass equal to $m_c = 1.5$ GeV. There is also quark contribution in the form of the second term in Eq. (22) which is proportional to F_2. We emphasize
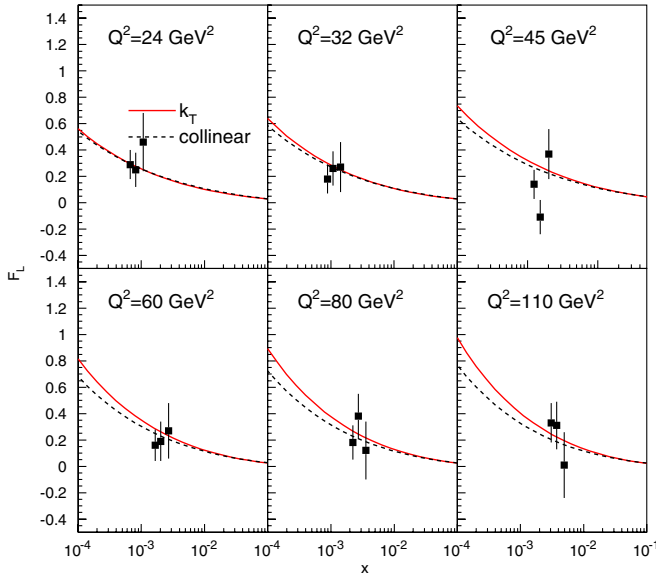

FIG. 5 (color online).   Comparison between the collinear and the k_T factorization calculations with exact gluon kinematics. The data are from the ZEUS experiment [2]. The light quarks u, d, s are treated as massless, and the charm quark mass is set to be $m_c = 1.5$ GeV. The solid (red) line denotes the calculation using the k factorization with exact kinematics, the dashed (black) line is the calculation using the collinear factorization with the massive charm quark.
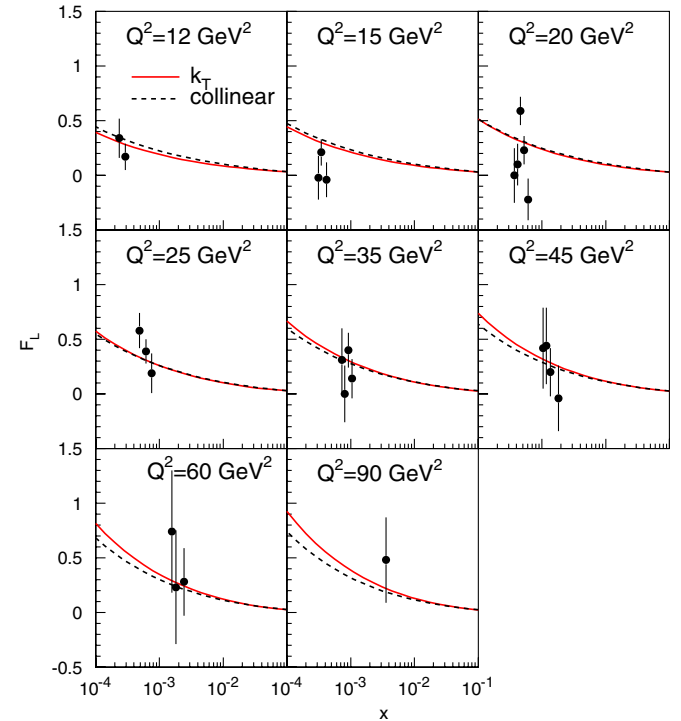
FIG. 6 (color online).   Comparison between the collinear and the k_T factorization calculations with exact gluon kinematics. The data are from the H1 experiment [1]. The light quarks u, d, s are treated as massless, and the charm quark mass is set to be $m_c = 1.5$ GeV. The solid (red) line denotes the calculation using the k_T factorization with exact kinematics, the dashed (black) line is the calculation using the collinear factorization with the massive charm quark.

that we have fitted only the F_2 data, thus the calculations for F_L are then the absolute predictions.

In Figs. 5 and 6 we show the calculations obtained using the collinear approach and the results from the k_T factorization formalism with the exact kinematics. The F_L structure function is plotted as a function of x in bins of Q^2. The data shown in Figs. 5 and 6 are from ZEUS [2] and H1 [1] experiments, respectively. The agreement between the experimental data and our calculations is good. In the case of the k_T factorization with the exact kinematics the results are rather close to the ones obtained from the collinear approach. For the kinematics range of the HERA data we do not see any significant differences for F_L between these two different factorization schemes. The only regions where the results differ is the region of very small x and high Q^2, where the k_T factorization with exact kinematics tends to give higher values, and the region of small Q^2 (below 10 GeV^2) where the k_T factorization-based approach falls below collinear one (compare Fig. 3). This result is consistent with the previous observations [40] which show that the significant difference between the high energy and the collinear factorizations is more pronounced for the transverse structure function [12].

We stress, though, the importance of the exact kinematics in the evaluation of the gluon density. The collinear and k_T factorization approaches give very similar results only in the case when the gluon density is evaluated at x_g in the k_T factorization formula. In Figs. 7 and 8 we show also the
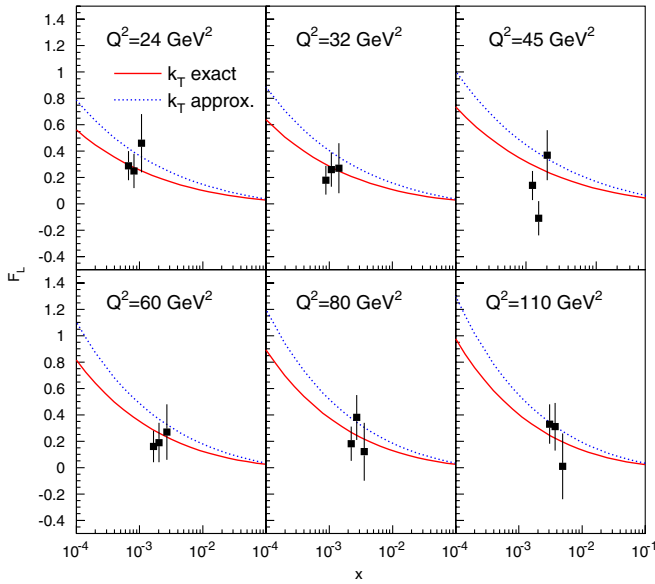

FIG. 8 (color online). Comparison between the exact and the approximate (dipolelike) kinematics in the k_T factorization formula. The data are from the H1 experiment [1]. The light quarks u, d, s are treated as massless, and the charm quark mass is set to be $m_c = 1.5$ GeV. The solid (red) line denotes the calculation using the k_T factorization with exact kinematics; the dotted (blue) line is the calculation using the k_T factorization with the approximate (dipolelike) kinematics.
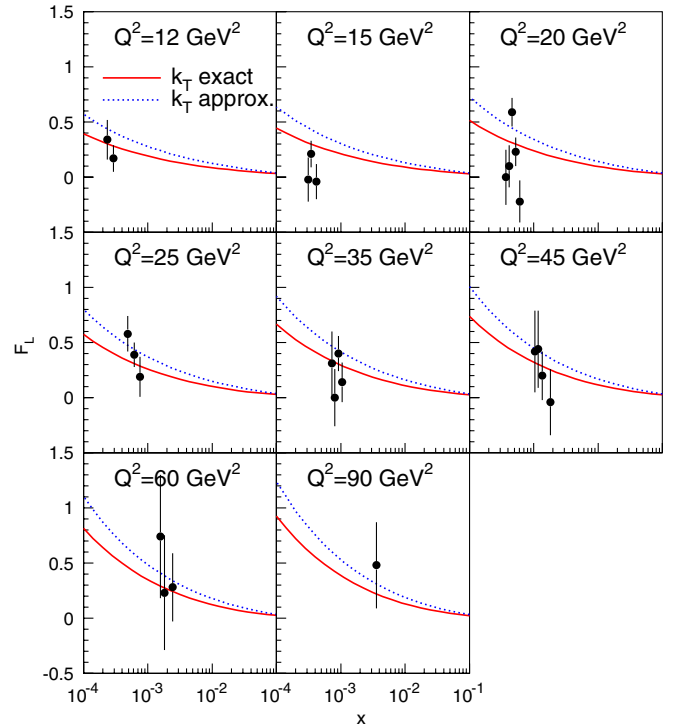

FIG. 7 (color online). Comparison between the exact and the approximate (dipolelike) kinematics in the k_T factorization formula. The data are from the ZEUS experiment [2]. The light quarks u, d, s are treated as massless, and the charm quark mass is set to be $m_c = 1.5$ GeV. The solid (red) line denotes the calculation using the k_T factorization with exact kinematics; the dotted (blue) line is the calculation using the k_T factorization with the approximate kinematics.

calculation where in the k_T factorization the argument of the gluon density equals the Bjorken x. Clearly, the results which do not take into account the exact kinematics are much higher than those with the exact kinematics. This is understandable as we are taking into account that finite energy has been used for the production of the $q\bar{q}$ pair, and as a result the argument of the gluon density $x_g > x$. We see that the differences are quite pronounced, they are typically larger than the differences between the collinear and the k_T factorization with the exact kinematics. The differences are also visible in the plots of F_L as a function of Q^2. It is interesting that the differences do not seem to vanish as a function of Q^2. This difference can be of course accounted for by changing the gluon density. The results for the F_L and F_2 structure functions can be made consistent within the two calculations (with and without exact kinematics) at the expense of having different normalizations for the gluon density.

We have checked that the contribution from the k_T factorization which is proportional to the gluon density is about 2–4 times smaller with the exact kinematics than the approximate calculation. We have found that the approximate kinematics yields similar results when $x_g \simeq 5.7x$ with
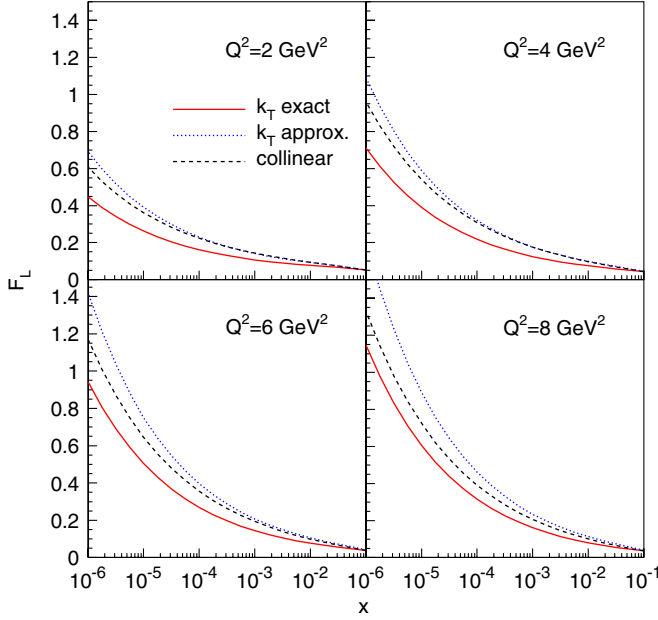
FIG. 9 (color online). Comparison between the collinear and the k_T factorization calculations for low values of Q^2. The range in x covers the LHeC kinematic range. The light quarks u, d, s are treated as massless, and the charm quark mass is set to be $m_c = 1.5$ GeV. The solid (red) line denotes the calculation using the k_T factorization with exact kinematics; the dotted (blue) line is the calculation using the k_T factorization with approximate kinematics; and the dashed (black) line is the calculation using the collinear factorization.

the proportionality coefficient being the slowly varying function of Q^2.

In Fig. 9 we present the comparison of the k_T and collinear factorizations for low values of $Q^2 \approx 2$–8 GeV^2. We see that the two computations differ more in this region. The lowest values are given by the k_T factorization approach with the exact kinematics while the highest values are given by the calculations with an approximate kinematics. At the lowest bin, $Q^2 = 2$ GeV^2, the differences seem to be smaller. This is due to the fact that in this region the calculation is dominated by the contribution of the quarks and the nonperturbative input which is the same in the k_T and the collinear factorization formulas in our approach. The range in x has been extended down to $x = 10^{-6}$ to cover the LHeC kinematic region.

In the lowest Q^2 region the quark contribution and the nonperturbative gluonic component becomes dominant. This is why the differences between the exact and the

approximate kinematics are starting to become smaller in this region as the whole F_L gets a larger contribution from the quarks which are treated in the same way in both of these calculations.

In the larger x region, below 10^{-3}, we observe that the kinematical effects are more significant. Interestingly, the gluon contribution originating from $k_T > k_0$ at $x \simeq 0.01$ is very small for the scales Q^2 up to about 10 GeV^2 and this region is completely dominated by the quark and the nonperturbative contribution. Therefore, using the approximate kinematics leads to large overestimation of the perturbative gluon contribution in this region.

VI. CONCLUSIONS

In this paper we have computed the longitudinal structure function F_L of the proton within the k_T factorization framework, using the unified BFKL/DGLAP resummation scheme for the unintegrated gluon density. Since we have only fitted our parameters to the F_2 data, the calculations for F_L are absolute predictions. The calculations are consistent with the experimental data from the HERA collider.

We have analyzed the impact of the exact kinematics in the k_T factorization scheme. The exact gluon kinematics is very important for the phenomenological description of the data on F_L. In particular, it leads to larger differences than changing from the k_T factorization to the collinear factorization scheme, at least in the available kinematical region of the HERA data.

We have also shown that the k_T factorization scheme with exact kinematics includes both the collinear and the dipole limits. The first one is recovered by assuming the strong ordering in the gluon and quark momenta, together with the exact gluon kinematics. The latter one is recovered in the limit when the fraction of the gluon's longitudinal momentum is set to be equal to Bjorken x.

The precision of the available HERA data for F_L does not allow to uniquely discriminate between different approaches. It is possible, however, that by lowering the value of Q^2 or extending the kinematic regime to lower values of x (like in the proposed LHeC collider) one can explore the differences between the presented frameworks.

ACKNOWLEDGMENTS

[1] F. D. Aaron *et al.* (H1 Collaboration), Phys. Lett. B **665,** 139 (2008).

[2] ZEUS Collaboration, DESY Report No. DESY-09-046, 2009.

[3] S. Catani, M. Ciafaloni, and F. Hautmann, Phys. Lett. B **242**, 97 (1990).

[4] J. C. Collins and R. K. Ellis, Nucl. Phys. **B360**, 3 (1991).

[5] V. S. Fadin, E. A. Kuraev, and L. N. Lipatov, Phys. Lett. **60B**, 50 (1975).

[6] L. N. Lipatov, Sov. J. Nucl. Phys. **23**, 338 (1976).

[7] I. I. Balitsky and L. N. Lipatov, Sov. J. Nucl. Phys. **28**, 822 (1978).

[8] M. Ciafaloni, Nucl. Phys. **B296**, 49 (1988).

[9] S. Catani, F. Fiorani, and G. Marchesini, Phys. Lett. B **234**, 339 (1990).

[10] S. Catani, F. Fiorani, and G. Marchesini, Nucl. Phys. **B336**, 18 (1990).

[11] G. Marchesini, Nucl. Phys. **B445**, 49 (1995).

[12] J. Kwiecinski, A. D. Martin, and A. M. Stasto, Phys. Rev. D **56**, 3991 (1997).

[13] V. N. Gribov and L. N. Lipatov, Sov. J. Nucl. Phys. **15**, 438 (1972).

[14] G. Altarelli and G. Parisi, Nucl. Phys. **B126**, 298 (1977).

[15] Y. L. Dokshitzer, Sov. Phys. JETP **46**, 641 (1977).

[16] M. Klein, in *Proceedings of the 16th International Workshop on Deep Inelastic Scattering and Related Subjects (DIS 2008), London, England, 7–11 April 2008* (Science Wise, 2008), doi:10.3360/dis.2008.20.

[17] A. Bialas, H. Navelet, and R. B. Peschanski, Nucl. Phys. **B593**, 438 (2001).

[18] A. Bialas, H. Navelet, and R. B. Peschanski, Nucl. Phys. **B603**, 218 (2001).

[19] J. C. Collins, T. C. Rogers, and A. M. Stasto, Phys. Rev. D **77**, 085009 (2008).

[20] L. N. Lipatov, Sov. Phys. JETP **63**, 904 (1986).

[21] V. S. Fadin and L. N. Lipatov, Phys. Lett. B **429**, 127 (1998).

[22] M. Ciafaloni and G. Camici, Phys. Lett. B **430**, 349 (1998).

[23] G. Camici and M. Ciafaloni, Phys. Lett. B **412**, 396 (1997).

[24] B. Andersson, G. Gustafson, H. Kharraziha, and J. Samuelsson, Z. Phys. C **71**, 613 (1996).

[25] J. Kwiecinski, A. D. Martin, and P. J. Sutton, Z. Phys. C **71**, 585 (1996).

[26] G. P. Salam, J. High Energy Phys. 07 (1998) 019.

[27] M. Ciafaloni, D. Colferai, G. P. Salam, and A. M. Stasto, Phys. Rev. D **66**, 054014 (2002).

[28] M. Ciafaloni, D. Colferai, G. P. Salam, and A. M. Stasto, Phys. Lett. B **541**, 314 (2002).

[29] M. Ciafaloni, D. Colferai, G. P. Salam, and A. M. Stasto, J. High Energy Phys. 08 (2007) 046.

[30] G. Altarelli, R. D. Ball, and S. Forte, Nucl. Phys. **B575**, 313 (2000).

[31] G. Altarelli, R. D. Ball, and S. Forte, Nucl. Phys. **B599**, 383 (2001).

[32] G. Altarelli, R. D. Ball, and S. Forte, Nucl. Phys. **B621**, 359 (2002).

[33] G. Altarelli, R. D. Ball, and S. Forte, Nucl. Phys. **B742**, 1 (2006).

[34] A. Sabio Vera, Nucl. Phys. **B722**, 65 (2005).

[35] C. D. White and R. S. Thorne, Phys. Rev. D **75**, 034005 (2007).

[36] J. Bartels, K. Golec-Biernat, and H. Kowalski, Phys. Rev. D **66**, 014001 (2002).

[37] J. Bartels, K. J. Golec-Biernat, and K. Peters, Eur. Phys. J. C **17**, 121 (2000).

[38] K. Golec-Biernat and M. Wusthoff, Phys. Rev. D **59**, 014017 (1998).

[39] J. Bartels, K. Golec-Biernat, and L. Motyka (unpublished).

[40] B. Badelek, J. Kwiecinski, and A. Stasto, Z. Phys. C **74**, 297 (1997).